Progress In Electromagnetics Research, PIER 78, 329–347, 2008

FIELD ANALYSIS OF DIELECTRIC WAVEGUIDE DEVICES BASED ON COUPLED TRANSVERSE-MODE INTEGRAL EQUATION — MATHEMATICAL AND NUMERICAL FORMULATIONS

H.-W. Chang

Institute of Electro-optical Engineering
National Sun Yat-sen University
Kaohsiung 80424, Taiwan

M.-H. Sheng

Department of Management Information Science
Chia Nan University of Pharmacy & Science
Tainan 71710, Taiwan

Abstract—We propose an integral-equation formulation for analyzing EM field of 2-D dielectric waveguide devices. The complex 2-D device is first divided into slices of 1-D horizontally layered structures. The entire EM solutions are determined by transverse field functions on the interfaces between slices. These functions are governed by a system of integral equations whose kernels are constructed from layer modes of each slice. These unknown tangential field functions are expanded as some linear combination of known basis functions. Various waveguide devices such as multi-mode interferometers, waveguide crossing and quasi-adiabatic tapered waveguides can be formulated and studied using present formulation.

1. INTRODUCTION

Dielectric waveguides devices are important building blocks in modern optical communication systems [1, 2]. The working principles of these passive dielectric waveguide devices are based on all EM wave physics, including propagation, reflection, transmission, diffraction, scattering, interferencing and so on [3]. These device structures are very large with a typical dimension of a few millimeters to a few centimeters. Improved electromagnetic theory and computational

methods are needed to handle the challenge of modeling these large passive waveguides and devices. A 3-D dielectric waveguide device has all six EM components. Their modes are in general complex and the field problems are intrinsically vectorial. Fortunately most 3-D devices can be approximated by their equivalent 2-D structures via effectively index averaging [4, 5] along the least important axis (typically the depth axis when the etching depth is very deep). 2-D dielectric waveguide problems are divided into TE and TM cases. The two cases are decoupled. Each can be treated as a scalar wave problem [6, 7]. For complex but compact optical devices, methods such as the finite-difference time-domain methods (FD-TD) [8–11], frequency-domain finite-difference methods (FD-FD) [12, 13] and the finite element method [14, 15] can be quite effective. For extremely large optical structures with smooth changing index profiles such as the adiabatic waveguides, the beam propagation method (BPM) and its variations [16, 17] are extensively used for field evolutions and mode profile determination. BPM methods apply a one-way approximation to the Maxwell's equations making it possible to advance the field solutions plane by plane along the propagation axis.

We present a coupled transverse-mode integral-equation (CTMIE) formulation [18–20], a generalization of the mode matching method (MMM) [21–23], to study bidirectional traffic inside a complex waveguide device. Like CTMIE, MMM employs the mode matching principle to match the continuity conditions at slice interface. The unknowns are the reflection/transmission coefficients in the first and last slice and standing wave coefficients in between. They satisfy a set of matrix equations. The unknown in CTMIE are the transverse-tangential field functions which satisfy exact coupled integral equations. This paper handles the background information and deals with the theoretical and numerical formulation of CTMIE. Real waveguide examples will be discussed in our future papers.

2. CTMIE THEORY

A general dielectric waveguide device is shown in Fig. 1. The original structure is divided into sections by a series of vertical cuts. Each section, called a slice, is then approximated by a horizontally layered dielectric waveguide. There are altogether $(N+1)$ slices and N vertical interfaces. The left end is the input waveguide while the right end is the exit waveguides. The formulation allows different boundary conditions, such as Dirichlet's B. C., Neumann's B. C., or Sommerfeld radiation conditions [6], at the right end of this structure which is terminated with either a perfectly electric/magnetic conducting

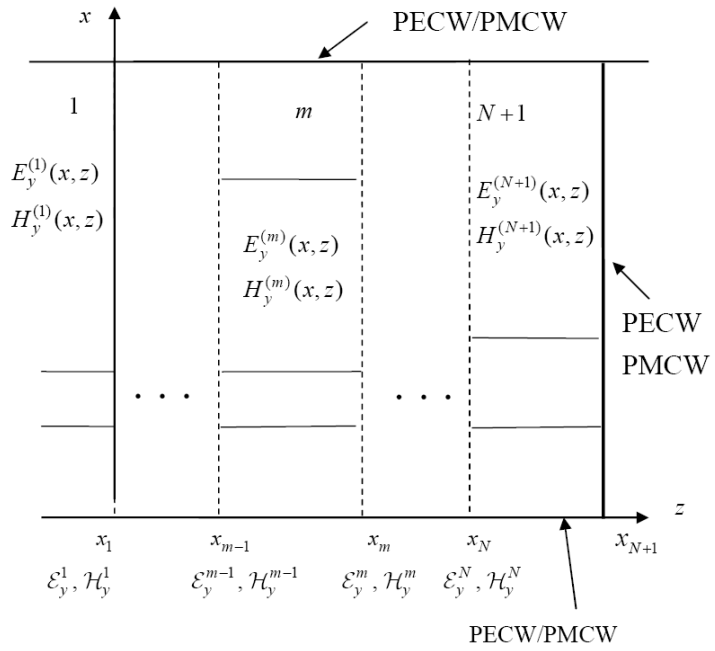

Figure 1. A General 2-D dielectric waveguide is divided to $(N+1)$ regions (slices) made of horizontally layered dielectric waveguides. For TE problems, the unknown functions are the tangential 1-D functions $\left\{\mathcal{E}_y^m(x)\right\}$, $m = 1, \cdots, N$ on the interfaces between two adjacent slices, whereas for TM problems, the unknowns are $\left\{\mathcal{H}_y^m(x)\right\}$, $m = 1, \cdots, N$. At the top bottom boundaries are PECW or PMCW. In the transmitted region, the boundary can be either PECW/ PMWC or be extended to infinity.

wall (PECW/PMCW) or a waveguide extended to infinity. To help discretizing the slice modes (layer modes), we place two PECWs at both the upper and lower boundaries. In cases that EM field may leak into the upper or lower part of the device, an artificial absorbing layer such as the PML [11, 24] can be added to reduce unwanted reflections from these artificial boundaries.

At the interface across two neighboring slices, the tangential field function $E_y(x,z)$ or $H_y(x,z)$ is required to be continuous. We shall denote these unknown interfacial field functions by the calligraphic letters $\mathcal{E}(x)$ and $\mathcal{H}(x)$ symbols. The other tangential component is the $H_x(x)$ for TE case and $E_x(x)$ for TM case. They can then be generated by taking the z-derivative of the $E_y(x,z)$ and $H_y(x,z)$

respectively. The continuity of these x-component functions will lead to coupled integral equations for all these $\mathcal{E}(x)$ or $\mathcal{H}(x)$ functions on all N interfaces. We shall denote the equations by coupled transverse-mode integral equation, or "CTMIE" for short. The simplest TMIE formulation for studying the scattering off a periodic grating can be found in chapter 7 of Ref. [6]. The application of TMIE to the dielectric waveguide termination problems can be found in Ref. [18] in which the authors first coined the term "TMIE". The 3-D version of CTMIE called VCTMIE was used to compute vector modes of complex rectangular-like dielectric waveguides [19, 20].

It is well-known that differential equations for these TE and TM slice modes can be formulated in Sturm-Liouville form [7], and thus they are orthonormal. By writing TE mode of $E_y(x,z)$ and TM mode of $H_y(x,z)$ as $\phi_e(x)\exp(-j\beta z)$ and $\phi_h(x)\exp(-j\beta z)$, we obtain the following differential equations for the TE eigenfunction $\phi_e(x)$ and TM eigenfunction $\phi_h(x)$:

$$\begin{aligned} \phi_e''(x) + k_0^2\epsilon_r(x)\phi_e(x) &= \lambda_e\phi_e(x), \\ \int \phi_{e,i}(x)\frac{1}{\mu_r(x)}\left[\phi_{e,i}\right]^* dx &= \delta_{i,j} \end{aligned} \tag{1a}$$

$$\begin{aligned} \left[\frac{\phi_h'(x)}{\epsilon_r(x)}\right]' + k_0^2\phi_h(x) &= \lambda_h\frac{\phi_h(x)}{\epsilon_r(x)}, \\ \int \phi_{h,i}(x)\frac{1}{\varepsilon_r(x)}\left[\phi_{h,i}\right]^* dx &= \delta_{i,j} \end{aligned} \tag{1b}$$

where k_0 is the wavenumber in a vacuum and x-dependent $\epsilon_r(x)$ is the relative dielectric constant within each slice. The relative permeability constant μ_r is assumed to be unity. The single 'prime' denotes the first derivative with respect to x. Here, β is the propagation constant within each slice.

To derive CTMIE, let us consider the TM case first. The TE case is a simplification of the TM case for dielectric media with constant permeability μ_0. For TM modes, the transverse magnetic field intensity functions in each slice can be written as a linear combination of the slice layer mode solution. In the incident region, we have both incident wave and reflected waves which can be written as:

$$\begin{aligned} H_y^{(1)}(x,z) \;=\; & \phi_i^{(1)}(x)e^{-j\beta_i^{(1)}(z-z_1)} \\ & + \sum_n r_n'\phi_n^{(1)}(x)e^{j\beta_n^{(1)}(z-z_1)}, \quad z < z_1 \end{aligned} \tag{2a}$$

Here we assume that the incident field is the ith mode in the input waveguide. To facilitate CTMIE derivation, we shall combine the incident wave with a 100% reflected wave of the same mode. Thus we have

$$\begin{aligned} H_y^{(1)}(x,z) &= -2j\phi_i^{(1)}(x)\sin\beta_i^{(1)}(z-z_1) \\ &\quad + \sum_n r'_n\phi_n^{(1)}(x)e^{j\beta_i^{(1)}(z-z_1)}, \quad z<z_1 \end{aligned} \tag{2b}$$

The reflection coefficient r' is related to the unprimed r_n by

$$\begin{aligned} r_n &= r'_n \qquad \text{if} \qquad n\neq i \\ r_n &= r'_n - 1 \qquad \text{if} \qquad n=i. \end{aligned} \tag{2c}$$

For slice $m,\ 1<m<N+1$ corresponding to waves in the scattering regions, the complete field solutions are made of both forward and backward traveling slice modes:

$$\begin{aligned} H_y^{(m)}(x,z) =& \sum_n \hat{a}_n^{(m)}\phi_n^{(m)}(x)\exp\left[-j\beta_n^{(m)}(z-z_{m-1})\right] \\ &+\sum_n \hat{b}_n^{(m)}\phi_n^{(m)}(x)\exp\left[-j\beta_n^{(m)}(z_m-z)\right],\ z_{m-1}<z<z_m \end{aligned} \tag{3a}$$

They can be written in terms of sine and cosine functions, or in terms of the following two shifted normalized sine functions (SNS) as

$$\begin{aligned} H_y^{(m)}(x,z) =& \sum_n a_n^{(m)}\phi_n^{(m)}(x)\frac{\sin\beta_n^{(m)}(z_m-z)}{\sin\left(\beta_n^{(m)}\Delta z_m\right)} \\ &+b_n^{(m)}\phi_n^{(m)}(x)\frac{\sin\beta_n^{(m)}(z-z_{m-1})}{\sin\left(\beta_n^{(m)}\Delta z_m\right)},\ \Delta z_m = z_m - z_{m-1}. \end{aligned} \tag{3b}$$

Fields in the last slice (slice $N+1$), with an output waveguide that extends to infinity (transparent boundary condition, TBC), we have

$$\begin{aligned} H_y^{(N+1)}(x,z) &= \sum_n t_n\phi_n^{(N+1)}(x)e^{-j\beta_n^{(N+1)}(z-z_N)}, \quad z>z_N \\ \mathcal{H}^{(N)}(x) &= H_y^{(N+1)}(x,z_1) = \sum_n t_n\phi_n^{(N+1)}(x) \end{aligned} \tag{3c}$$

For PMCW (TM case, magnetic wall)

$$H_y^{(N+1)}(x,z) = \sum_n t_n \phi_n^{(N+1)}(x) \frac{\sin \beta_n^{(N+1)} (z_{N+1} - z)}{\sin \beta_n^{(N+1)} \Delta z_{N+1}}, \tag{3d}$$
$$\Delta z_{N+1} = z_{N+1} - z_N$$

For PECW case, (TM case, electric wall)

$$H_y^{(N+1)}(x,z) = \sum_n t_n \phi_n^{(N+1)}(x) \frac{\cos \beta_n^{(N+1)} (z_{N+1} - z)}{\cos \beta_n^{(N+1)} \Delta z_{N+1}}. \tag{3e}$$

Equation (3b) remains valid as long as the two identical denominators $\sin\left(\beta_n^{(m)} \Delta z_m\right)$ remain non-zero. The advantages of using the SNS are that one can easily verify that at $z = z_{m-1}$

$$\mathcal{H}^{(m-1)}(x) = H_y^{(m)}(x, z_{m-1}) = \sum_n a_n^{(m)} \phi_n^{(m)}(x), \tag{4a}$$

and at $z = z_m$

$$\mathcal{H}^{(m)}(x) = H_y^{(m)}(x, z_m) = \sum_n b_n^{(m)} \phi_n^{(m)}(x), \quad 1 \le m \le N \tag{4b}$$

For the same reason, we define r_n in such a way that the first unknown transverse field function $\mathcal{H}^{(1)}(x)$ which is given by

$$\mathcal{H}^{(1)}(x) = H_y^{(1)}(x, z_1) = \sum_n r_n \phi_n^{(1)}(x), \tag{4c}$$

is completely made of reflection wave fields. The reflection coefficients are obtained via the following integration using the orthonormal property of the eigenfunctions:

$$r_n = \int_{-\infty}^{\infty} \mathcal{H}^{(1)}(x) \frac{1}{\varepsilon_r^{(1)}(x)} \phi_n^{*(1)}(x)\, dx, \tag{5a}$$

Likewise the SNS coefficients as well as the transmission coefficients can be obtain

$$\begin{aligned} a_n^{(m)} &= \int_{-\infty}^{\infty} \mathcal{H}^{(m-1)}(x) \frac{1}{\varepsilon_r^{(m)}(x)} \phi_n^{*(m)}(x) dx, \\ b_n^{(m)} &= \int_{-\infty}^{\infty} \mathcal{H}^{(m)}(x) \frac{1}{\varepsilon_r^{(m)}(x)} \phi_n^{*(m)}(x) dx, \end{aligned} \tag{5b}$$

and

$$t_n = \int_{-\infty}^{\infty} \mathcal{H}^{(N)}(x) \frac{1}{\varepsilon_r^{(N)}(x)} \phi_n^{*(N)}(x) dx. \tag{5c}$$

Given Eqs. (1a)–(3e) for the tangential magnetic field $H_y(x,z)$, we can obtain the tangential electric field intensity $E_x(x,z)$ as

$$\begin{aligned} E_x^{(1)}(x,z) &= \frac{-1}{\omega\varepsilon^{(1)}(x)} \left\{ 2\beta_i^{(1)} \phi_i^{(1)}(x) \cos\beta_i^{(1)}(z-z_1) \right. \\ &\quad \left. - \sum_n \beta_n^{(1)} r_n \phi_n^{(1)}(x) e^{j\beta_n^{(1)}(z-z_1)} \right\}. \end{aligned} \tag{6a}$$

$$\begin{aligned} E_x^{(m)}(x,z) &= \frac{j}{\omega\varepsilon^{(m)}} \left\{ \sum_n \beta_n^{(m)} a_n^{(m)} \phi_n^{(m)}(x) \frac{\cos\beta_n^{(m)}(z_m - z)}{\sin\left(\beta_n^{(m)} \Delta z_m\right)} \right. \\ &\quad \left. -\beta_n^{(m)} b_n^{(m)} \phi_n^{(m)}(x) \frac{\cos\beta_n^{(m)}(z - z_{m-1})}{\sin\left(\beta_n^{(m)} \Delta z_m\right)} \right\} \end{aligned} \tag{6b}$$

Finally, in the last region, first the TBC case,

$$E_x^{(N+1)}(x,z) = \frac{-1}{\omega\varepsilon^{(N+1)}(x)} \sum_n \beta_n^{(N+1)} t_n \phi_n^{(N+1)}(x) \cdot \psi_h(z), \tag{6c}$$

where

$$\psi_h(z) = \begin{cases} e^{-j\beta_n^{(N+1)}(z-z_N)}, & \text{(TBC)} \\ \dfrac{-\cos\beta_n^{(N+1)}(z_{N+1}-z)}{\sin\beta_n^{(N+1)} z_{N+1}}, & \text{(TM, PEMW)} \\ \dfrac{\sin\beta_n^{(N+1)}(z_{N+1}-z)}{\cos\beta_n^{(N+1)} \Delta z_{N+1}}, & \text{(TM, PECW)} \end{cases} \tag{6d}$$

We can represent the entire 2-D field $E_x(x,z)$ in term of a set of unknown functions $\left\{\mathcal{H}_{(m)}(x)\right\}$, $m = 1, \cdots, N$. But first, we need to define TM mode impedance and Green's operators

$$\eta_n^{(m)} \triangleq \frac{E_x^{(m)}}{H_y^{(m)}} = \frac{\beta_n^{(m)}}{\omega\varepsilon_0} \qquad m = 1 \ldots N+1, \quad \text{(TM impedance)} \tag{7a}$$

The Green's operator takes a magnetic function and transforms it to an electric field function via integration:

$$E_x(x,z) = \int G(x,x',z) H_y(x,z) dx'.$$

In the input waveguide, we have

$$\begin{aligned} E_x^{(1)}(x,z) &= -2\eta_i^{(1)} \frac{\phi_i^{(1)}(x)}{\varepsilon_r^{(1)}(x)} \cos\beta_i^{(1)}(z-z_1) + \int \mathbf{G}_h^{(1)} \mathcal{H}_1(x') dx' \\ \mathbf{G}_h^{(1)}(x,x',z) &= \sum_n \eta_n^{(1)} \frac{\phi_n^{(1)}(x)}{\varepsilon_r^{(1)}(x)} \frac{\phi_n^{*(1)}(x')}{\varepsilon_r^{(1)}(x')} e^{j\beta_n^{(1)}(z-z_1)} \end{aligned} \tag{7b}$$

In the middle regions, we have

$$\begin{aligned} E_x^{(m)}(x,z) &= \int \mathbf{G}_h^{(m,l)} \mathcal{H}_{m-1}(x') dx' + \int \mathbf{G}_h^{(m,r)} \mathcal{H}_m(x') dx', \\ \mathbf{G}_h^{(m,l)}(x,x',z) &= j \sum_n \eta_n^{(m)} \frac{\phi_n^{(m)}}{\varepsilon_r^{(m)}} \frac{\phi_n^{*(m)}(x')}{\varepsilon_r^{(m)}(x')} \frac{\cos\beta_n^{(m)}(z_m - z)}{\sin\left(\beta_n^{(m)} \Delta z_m\right)}, \\ \mathbf{G}_h^{(m,r)}(x,x',z) &= -j \sum_n \eta_n^{(m)} \frac{\phi_n^{(m)}}{\varepsilon_r^{(m)}} \frac{\phi_n^{*(m)}(x')}{\varepsilon_r^{(m)}(x')} \frac{\cos\beta_n^{(m)}(z - z_{m-1})}{\sin\left(\beta_n^{(m)} \Delta z_m\right)}. \end{aligned} \tag{7c}$$

In the last region, we have

$$\begin{aligned} E_x^{(N+1)}(x,z) &= \int \mathbf{G}_h^{(N+1)}(x,x',z) \mathcal{H}_N(x') dx' \\ \mathbf{G}_h^{(N+1)}(x,x',z) &= \sum_n \eta_n^{(N+1)} \frac{\phi_n^{(N+1)}}{\varepsilon_r^{(N+1)}} \frac{\phi_n^{*(N+1)}(x')}{\varepsilon_r^{(N+1)}(x')} \psi_h(z), \end{aligned} \tag{7d}$$

In the expressions above, the asterisk (*) denotes the complex conjugate. Next, we will further classify the two Green's operators (Equation (7c)) in the middle regions into four operators

$$\begin{aligned} \mathbf{P}_h^{(m)} &= \mathbf{G}_h^{(m,l)}(z_m) = j \sum_{n=1}^{\infty} \eta_n^{(m)} \frac{\phi_n^{(m)}(x)}{\varepsilon_r^{(m)}(x)} \frac{\phi_n^{*(m)}(x')}{\varepsilon_r^{(m)}(x')} \csc(\beta_n^{(m)} \Delta z_m) \\ \mathbf{Q}_h^{(m)} &= \mathbf{G}_h^{(m,l)}(z_{m-1}) = j \sum_{n=1}^{\infty} \eta_n^{(m)} \frac{\phi_n^{(m)}(x)}{\varepsilon_r^{(m)}(x)} \frac{\phi_n^{*(m)}(x')}{\varepsilon_r^{(m)}(x')} \cot(\beta_n^{(m)} \Delta z_m) \end{aligned}$$

$$\mathbf{R}_h^{(m)} = \mathbf{G}_h^{(m,r)}(z_m) = -j\sum_{n=1}^{\infty} \eta_n^{(m)} \frac{\phi_n^{(m)}(x)}{\varepsilon_r^{(m)}(x)} \frac{\phi_n^{*(m)}(x')}{\varepsilon_r^{(m)}(x')} \cot(\beta_n^{(m)} \Delta z_m)$$

$$\mathbf{S}_h^{(m)} = \mathbf{G}_h^{(m,r)}(z_{m-1}) = -j\sum_{n=1}^{\infty} \eta_n^{(m)} \frac{\phi_n^{(m)}(x)}{\varepsilon_r^{(m)}(x)} \frac{\phi_n^{*(m)}(x')}{\varepsilon_r^{(m)}(x')} \csc(\beta_n^{(m)} \Delta z_m) \quad (8a)$$

$$\mathbf{S}_h^{(m)} = -\mathbf{P}_h^{(m)}, \quad \mathbf{Q}_h^{(m)} = -\mathbf{R}_h^{(m)}, \quad \eta_n^{(m)} = \frac{\beta_n^{(m)}}{\omega\varepsilon_0}$$

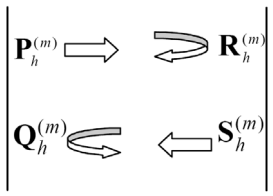

Figure 2. P Q R S Green's operators.

Figure 2 illustrates the physical significance of these four operators $\mathbf{P}_h^{(m)}$ operator "propagates" the left-interface source functions $\mathcal{H}_{m-1}(x)$ to the right-interface target function $\mathcal{E}_m(x)$. $\mathbf{Q}_h^{(m)}$ operator "back reflects" the left-interface source function $\mathcal{H}_{m-1}(x)$ to the right-interface target function $\mathcal{E}_m(x)$. $\mathbf{R}_h^{(m)}$ operator "reflects" the right source functions $\mathcal{H}_m$ to the left target function $\mathcal{E}_{m-1}$. $\mathbf{S}_h^{(m)}$: operator "back propagates" the right source function $\mathcal{H}_m$ to the left target function $\mathcal{E}_{m-1}$. The letter **P** is chosen for forward propagation and **R** is chosen for reflection from a forward wave. The letter **Q** and **S** are chosen for reflection and propagation in the backward direction. Note that letters "**P**, **Q**" go before letters "**R**, **S**" as the word "left" goes before the word "right". So we associated $\mathbf{P}_h^{(m)}$, $\mathbf{Q}_h^{(m)}$ operators with the left source function $\mathcal{H}_{m-1}$ while $\mathbf{R}_h^{(m)}$, $\mathbf{S}_h^{(m)}$ operators are associated with the right source function $\mathcal{H}_m$. This situation is further illustrated in Figure 2.

Using these four operators, we may express the two transverse electric field functions on the left and right boundaries of the mth slice in region m.

$$\begin{aligned} \mathcal{E}_{m-1}(x) &= E_x^{(m)}(x, z_{m-1}) = \int \mathbf{Q}_h^{(m)} \mathcal{H}_{m-1}(x')dx' + \int \mathbf{S}_h^{(m)} \mathcal{H}_m(x')dx', \\ \mathcal{E}_{m-1}(x) &= E_x^{(m)}(x, z_m) = \int \mathbf{P}_h^{(m)} \mathcal{H}_{m-1}(x')dx' + \int \mathbf{R}_h^{(m)} \mathcal{H}_m(x')dx' \end{aligned} \quad (8b)$$

Repeat this way for first and last regions, we have

$$\begin{aligned}\mathcal{E}_1(x) &= -2\eta_i^{(1)}\frac{\phi_i^{(1)}(x)}{\varepsilon_r^{(1)}(x)} + \int \mathbf{R}_h^{(1)}(x,x')\mathcal{H}_1(x')dx' \\ \mathbf{R}_h^{(1)}(x,x') &= \sum \eta_n^{(1)}\frac{\phi_n^{(1)}(x)}{\varepsilon_r^{(1)}(x)}\frac{\phi_n^{*(1)}(x')}{\varepsilon_r^{(1)}(x')}\end{aligned} \tag{8c}$$

$$\begin{aligned}\mathcal{E}_N(x) &= \int \mathbf{Q}_h^{(N+1)}(x,x')\mathcal{H}_N(x')dx' \\ \mathbf{Q}_h^{(N+1)}(x,x') &= \sum q_n^{(N+1)}\frac{\phi_n^{(N+1)}(x)}{\varepsilon_r^{(N+1)}(x)}\frac{\phi_n^{*(N+1)}(x')}{\varepsilon_r^{(N+1)}(x')} \\ q_n^{(N+1)} &= \begin{cases}\eta_n^{(N+1)}, & \text{TBC} \\ -j\eta_n^{(N+1)}\cot\left(\beta_k^{(i)}\Delta z_{N+1}\right), & \text{TM, PMCW} \\ j\eta_n^{(N+1)}\tan\left(\beta_k^{(i)}\Delta z_{N+1}\right), & \text{TE, PECW}\end{cases}\end{aligned} \tag{8d}$$

Up to now, we have not imposed any condition onto the N unknown tangential magnetic fields $\{\mathcal{H}_m(x)\}$, $m = 1, \cdots, N$. We know that given these 1-D functions $\{\mathcal{H}_m\}$, we are able to write the entire 2-D vector field functions within each region. We are able, in particular, write the tangential electric field at the slice interfaces $\{\mathcal{E}_m(x)\}$, $m = 1, \cdots, N$ in terms of $\{\mathcal{H}_m(x)\}$ using Eqs. (8c)–(8d). The continuity conditions of these tangential electric fields $\{\mathcal{E}_m(x)\}$ lead to the following coupled integral equations for the unknown functions $\{\mathcal{H}_m(x)\}$. We will derive these CTMIEs for following various cases:

Case $N = 1$:

For this case, there are only two operators involved. Thus we have:

$$\begin{aligned}\int dx'\mathbf{R}_h^{(1)}(x,x')\cdot\mathcal{H}_1(x') &= \int dx'\mathbf{Q}_h^{(2)}(x,x')\cdot\mathcal{H}_1(x') + 2\mathcal{E}_{\text{inc}}(x) \\ &\Rightarrow \int dx'\mathbf{G}_{1,1}(x,x')\cdot\mathcal{H}_1(x') = 2\mathcal{E}_{\text{inc}}(x), \quad \text{(9a)} \\ \mathbf{G}_{1,1}(x,x') &= \mathbf{R}_h^{(1)}(x,x') - \mathbf{Q}_h^{(2)}(x,x'),\end{aligned}$$

where the incident transverse electric field is given by

$$\mathcal{E}_{\text{inc}}(x) = \frac{\beta_i^{(1)}}{\omega\varepsilon^{(1)}(x)}\phi_i^{(1)}(x) = \eta_i^{(1)}\frac{\phi_i^{(1)}(x)}{\varepsilon_r^{(1)}(x)}. \tag{9b}$$

Note that except for the $\mathbf{Q}_h^{(2)}$ operator which is located in the last region and is given by Eq. (8d), all other operators are given by Eq. (8a).

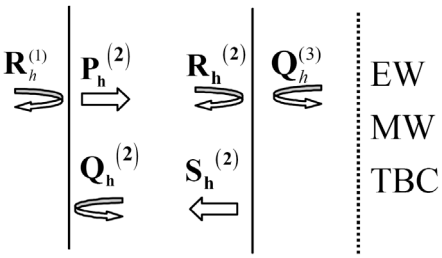

Figure 3. CTMIE operators for $N = 2$ case.

Case $N = 2$:

For this case, there are six operators involved as indicated in Figure 3. We can write one equation for equating the two adjacent tangential electric fields on each of the two vertical lines. Thus we have:

$$\begin{aligned} &\int dx' \begin{bmatrix} \mathbf{R}_h^{(1)}(x,x') & 0 \\ \mathbf{P}_h^{(2)}(x,x') & \mathbf{R}_h^{(2)}(x,x') \end{bmatrix} \begin{bmatrix} \mathcal{H}_1(x') \\ \mathcal{H}_2(x') \end{bmatrix} \\ &= \int dx' \begin{bmatrix} \mathbf{Q}_h^{(2)}(x,x') & \mathbf{S}_h^{(2)}(x,x') \\ 0 & \mathbf{Q}_h^{(3)}(x,x') \end{bmatrix} \begin{bmatrix} \mathcal{H}_1(x') \\ \mathcal{H}_2(x') \end{bmatrix} + \begin{bmatrix} 2\mathcal{E}_{\text{inc}}(x) \\ 0 \end{bmatrix} \end{aligned} \tag{9c}$$

This leads to the following two by two matrix operators:

$$\begin{aligned} &\int dx' \begin{bmatrix} \mathbf{G}_{1,1}(x,x') & \mathbf{G}_{1,2}(x,x') \\ \mathbf{G}_{2,1}(x,x') & \mathbf{G}_{2,2}(x,x') \end{bmatrix} \begin{bmatrix} \mathcal{H}_1(x') \\ \mathcal{H}_2(x') \end{bmatrix} = \begin{bmatrix} 2\mathcal{E}_{\text{inc}}(x) \\ 0 \end{bmatrix} \\ &\mathbf{G}_{1,1} = \mathbf{R}_h^{(1)} - \mathbf{Q}_h^{(2)}, \qquad \mathbf{G}_{1,2} = -\mathbf{S}_h^{(2)} \\ &\mathbf{G}_{2,1} = \mathbf{P}_h^{(2)}, \qquad \mathbf{G}_{2,2} = \mathbf{R}_h^{(2)} - \mathbf{Q}_h^{(3)} \end{aligned} \tag{9d}$$

Note that operator $\mathbf{Q}_h^{(3)}$ located in the last region is given by Eq. (8d)

Cases $N >= 3$:

For complex waveguide devices, we may use $N + 1 >= 4$ slices to approximate the underlying device. This will lead to the following

CTMIE equation with an $N \times N$ matrix operator, G

$$\int dx' \begin{bmatrix} \mathbf{G}_{1,1} & \mathbf{G}_{1,2} & 0 & \cdots & 0 \\ \vdots & \ddots & \vdots & \cdots & 0 \\ \cdots & \cdots & \mathbf{G}_{i,i} & \cdots & 0 \\ \vdots & \vdots & \vdots & \ddots & \vdots \\ 0 & \cdots & 0 & \mathbf{G}_{N,N-1} & \mathbf{G}_{N,N} \end{bmatrix} \begin{bmatrix} \mathcal{H}_1 \\ \vdots \\ \mathcal{H}_i \\ \vdots \\ \mathcal{H}_N \end{bmatrix} = \begin{bmatrix} 2\mathcal{E}_{\text{inc}} \\ \vdots \\ 0 \\ \vdots \\ 0 \end{bmatrix} \tag{10a}$$

Each of the matrix element is an operator given by

$$\begin{aligned} \mathbf{G}_{1,1} &= \mathbf{R}_h^{(1)} - \mathbf{Q}_h^{(2)}, \quad \mathbf{G}_{1,2} = -\mathbf{S}_h^{(2)} \\ \mathbf{G}_{i,i-1} &= \mathbf{P}_h^{(i)},\ \mathbf{G}_{i,i} = \mathbf{R}_h^{(i)} - \mathbf{Q}_h^{(i+1)},\ \mathbf{G}_{i,i+1} = -\mathbf{S}_h^{(i+1)},\ i = 1 \ldots N-1 \\ \mathbf{G}_{i+1,i} &= \mathbf{P}_h^{(i+1)}, \quad \mathbf{G}_{N,N-1} = \mathbf{P}_h^{(N)}, \quad \mathbf{G}_{N,N} = \mathbf{R}_h^{(N)} - \mathbf{Q}_h^{(N+1)}, \\ -\mathbf{S}_h^{(i)} &= \mathbf{P}_h^{(i)}, \quad \mathbf{G}_{i,i+1} = \mathbf{G}_{i+1,i}, \quad i = 1 \ldots N-1. \end{aligned} \tag{10b}$$

Thus we have completed the derivation of CTMIE for the TM cases. TE cases follow TM results directly if we replace all 2-D field functions $H_y(x,z)$ and $E_x(x,z)$ by $E_y(x,z)$ and $H_x(x,z)$, and we substitute all 1-D field functions $\mathcal{H}(x)$ by $\mathcal{E}(x)$. We also replace $\varepsilon(x)$ by μ_0 and change the TM wave impedance to the TE wave admittance. Furthermore, a left-handed coordinate system is assumed for the TE case to make the above rules work.

TE mode wave admittance is given below:

$$y_n^{(m)} \triangleq \frac{H_x^{(m)}}{E_y^{(m)}} = \frac{\omega\mu_0}{\beta_n^{(m)}} \qquad \text{(TE admittance)}. \tag{10c}$$

The definition of TM wave impedance is given by Eq. (7a). An additional subtle difference between TE and TM cases lies in handling three possible boundary conditions in the last region. In the last region, for TE case, we have:

$$\begin{aligned} H_z^{(N+1)}(x,z) &= \int \mathbf{G}_e^{(N+1)}(x,x',z)\mathcal{E}_N(x')dx' \\ \mathbf{G}_e^{(N+1)}(x,x',z) &= \sum_n y_n^{(N+1)}\phi_n^{(N+1)}\phi_n^{*(N+1)}(x')\psi_e(z), \end{aligned} \tag{10d}$$

where

$$\psi_e(z) = \begin{cases} e^{-j\beta_n^{(N+1)}(z-z_N)}, & \text{(TBC)}, \\ \dfrac{-\cos\beta_n^{(N+1)}(z_{N+1}-z)}{\sin\beta_n^{(N+1)} z_{N+1}}, & \text{(TE, PECW)} \\ \dfrac{\sin\beta_n^{(N+1)}(z_{N+1}-z)}{\cos\beta_n^{(N+1)}\Delta z_{N+1}}, & \text{(TE, PMCW)}. \end{cases}, \tag{10e}$$

Finally for TE case, $\mathcal{E}_{\text{inc}}$ in Eq. (10a) is replaced by the incident transverse magnetic field $\mathcal{H}_{\text{inc}}(x)$ given by

$$\mathcal{H}_{\text{inc}}(x) = \frac{\omega\mu_0}{\beta_i^{(1)}}\phi_i^{(1)}(x) = y_i^{(1)}\phi_i^{(1)}(x). \tag{11a}$$

We will also need to use the TE admittance for the last region:

$$q_n^{(N+1)} = \begin{cases} y_n^{(N+1)}, & \text{(TBC)} \\ -jy_n^{(N+1)}\cot\left(\beta_k^{(i)}\Delta z_{N+1}\right), & \text{(TE, PECW)} \\ jy_n^{(N+1)}\tan\left(\beta_k^{(i)}\Delta z_{N+1}\right), & \text{(TE, PMCW)} \end{cases} \tag{11b}$$

3. OVERLAP INTEGRAL

To obtain numerical solutions, we need to convert CTMIE Eqs. (10a)–(11a) into coupled matrix equations. First, the unknown 1-D tangential field functions $\{\mathcal{E}_i(x)\}$ and $\{\mathcal{H}_i(x)\}$ are expanded as linear combination of some known ortho-normal basis functions (for the choice of these basis functions please see Ref. [16]). Consider the TM case, let $N_b^{(i)}$ be the number of terms used to expand to ith unknown tangential field $\mathcal{H}_i(x)$, we write

$$\mathcal{H}_i(x) \cong \sum_{n=1}^{N_b^{(i)}} c_n^{(i)}\phi_n^{(i)}(x), \quad i = 1, \cdots, N. \tag{12a}$$

Next let us define the overlap integral of the ith unknown function $\mathcal{H}_i(x)$ and its adjacent slice modes in regions $i-1$ and i.

$$\begin{aligned} \boldsymbol{O}^{\bar{i},j} &= \left[O_{k,l}^{\bar{i},j}\right] = \left(\boldsymbol{O}^{j,\bar{i}}\right)^T, \quad j = i, i+1 \\ O_{k,l}^{\bar{i},j} &\triangleq \int \phi_k^{(i)}(x)\frac{1}{\varepsilon_r^{(j)}(x)}\phi_l^{(i)}(x)dx, \end{aligned} \tag{12b}$$

$$O_{k,l}^{j,\bar{i}} \triangleq \int \phi_l^{(i)}(x) \frac{1}{\varepsilon_r^{(j)}(x)} \phi_k^{(i)}(x)\, dx = O_{k,l}^{\bar{i},j}.$$

The bar on the superscript $\bar{i}$ denotes the unknown transverse function while the unbar superscript $j = (i, i-1)$ denote the jth slice. Matrices $\boldsymbol{O}^{\bar{i},j}$, $\boldsymbol{O}^{j,\bar{i}}$ are overlapped integral matrices. They are projection matrices result from projecting one orthonormal basis functions onto the other.

4. COUPLED MATRIX EQUATIONS

Using the previously defined overlap integral matrices, we then project Green's operators (in boldface roman font) in Eqs. (10a) and (11a) from their natural bases (slice modes) onto our chosen bases. The results are summarized in the following matrix representation of Green's operators (in boldface italic roman font).

$$\begin{aligned}
&\boldsymbol{G}_{i,i-1} \cdot \boldsymbol{c}_{i-1} + \boldsymbol{G}_{i,i} \cdot \boldsymbol{c}_i + \boldsymbol{G}_{i,i+1} \cdot \boldsymbol{c}_{i+1} = 0 \\
&\boldsymbol{G}_{i,i-1} = \boldsymbol{O}^{\bar{i},i} \boldsymbol{p}^{(i)} \boldsymbol{O}^{i,\overline{i-1}} \\
&\boldsymbol{G}_{i,i} = \boldsymbol{O}^{\bar{i},i} \boldsymbol{r}^{(i)} \boldsymbol{O}^{i,\bar{i}} - \boldsymbol{O}^{\bar{i},i+1} \boldsymbol{q}^{(i+1)} \boldsymbol{O}^{i+1,\bar{i}} \\
&\boldsymbol{G}_{i,i+1} = \boldsymbol{O}^{\bar{i},i+1} \boldsymbol{s}^{(i+1)} \boldsymbol{O}^{i+1,\overline{i+1}}.
\end{aligned} \tag{12c}$$

Lower-case boldface literals $\boldsymbol{p}\,\boldsymbol{q}\,\boldsymbol{r}\,\boldsymbol{s}$ are diagonal matrices given by

$$\begin{aligned}
\boldsymbol{p}^{(i)} &= \begin{bmatrix} p_1^{(i)} & \cdots & 0 \\ \vdots & p_k^{(i)} & \vdots \\ 0 & \cdots & p_M^{(i)} \end{bmatrix}, \quad \boldsymbol{s}^{(i)} = \begin{bmatrix} s_1^{(i)} & \cdots & 0 \\ \vdots & s_k^{(i)} & \vdots \\ 0 & \cdots & s_M^{(i)} \end{bmatrix}, \\
\boldsymbol{q}^{(i)} &= \begin{bmatrix} q_k^{(i)} & \cdots & 0 \\ \vdots & q_k^{(i)} & \vdots \\ 0 & \cdots & q_M^{(i)} \end{bmatrix}, \quad \boldsymbol{r}^{(i)} = \begin{bmatrix} r_k^{(i)} & \cdots & 0 \\ \vdots & r_k^{(i)} & \vdots \\ 0 & \cdots & r_M^{(i)} \end{bmatrix}, \\
p_k^{(i)} &= j\eta_k^{(i)} \csc\left(\beta_k^{(i)} \Delta z_i\right), \quad s_k^{(i)} = -j\,\eta_k^{(i)} \csc\left(\beta_k^{(i)} \Delta z_i\right), \\
q_k^{(i)} &= j\eta_k^{(i)} \cot\left(\beta_k^{(i)} \Delta z_i\right), \quad r_k^{(i)} = -j\,\eta_k^{(i)} \cot\left(\beta_k^{(i)} \Delta z_i\right),
\end{aligned} \tag{12d}$$

Note that the original Green's operators $\mathbf{P}\,\mathbf{Q}\,\mathbf{R}\,\mathbf{S}$ written in their natural bases are diagonal (Eqs. (8a), (11c)); however the projected matrix operators are in general dense and full except for the trivial cases of identical slices. The unknowns here are lowercase boldface

literals $\{c_i\}$, $i = 1, \cdots, N$. Final coupled matrix equations are

$$\begin{bmatrix} \boldsymbol{G}_{1,1} & \boldsymbol{G}_{1,2} & 0 & \cdots & 0 \\ \vdots & \ddots & \vdots & \cdots & 0 \\ 0 & \boldsymbol{G}_{i,i-1} & \boldsymbol{G}_{i,i} & \boldsymbol{G}_{i,i+1} & 0 \\ \vdots & \vdots & \vdots & \ddots & \vdots \\ 0 & \cdots & 0 & \boldsymbol{G}_{N,N-1} & \boldsymbol{G}_{N,N} \end{bmatrix} \begin{bmatrix} \boldsymbol{c}_1 \\ \vdots \\ \boldsymbol{c}_i \\ \vdots \\ \boldsymbol{c}_N \end{bmatrix} = \begin{bmatrix} 2\boldsymbol{b} \\ \vdots \\ 0 \\ \vdots \\ 0 \end{bmatrix}, \tag{12e}$$

The definition of $\mathbf{c}_i$ and the incident vector on the right hand side $\boldsymbol{b}$ are given by

$$c_i = \begin{bmatrix} c_1^{(i)} \\ \vdots \\ c_N^{(i)} \end{bmatrix}, \quad b = \begin{bmatrix} b_1^{(1)} \\ \vdots \\ b_N^{(1)} \end{bmatrix}, \quad b_k = \frac{\beta_i^{(1)}}{\omega} \int \phi_k^{(1)}(x) \frac{1}{\varepsilon_r^{(1)}} \phi_i^{(1)}(x) dx. \tag{12f}$$

In most cases, the incident mode is the fundamental mode ($i = 1$).

Once Eq. (12e) is solved for, the TM mode reflection and transmission coefficients of the waveguide device can be obtained via Eqs. (4c), (5a) and (12a) as

$$\Rightarrow \ \boldsymbol{r}'_h \triangleq \begin{bmatrix} r'_{h,1} \\ \vdots \\ r'_{h,M} \end{bmatrix}, \quad \boldsymbol{r}'_h = \boldsymbol{O}^{1,\bar{1}} \cdot \boldsymbol{c}_1, \quad \boldsymbol{t}_h \triangleq \begin{bmatrix} t_{h,1} \\ \vdots \\ t_{h,M} \end{bmatrix}, \quad \boldsymbol{t}_h = \boldsymbol{O}^{N+1,\bar{N}} \cdot \boldsymbol{c}_N, \tag{13a}$$

Similarly, coefficients for SNS in each region are given by

$$\begin{aligned} \boldsymbol{a}^{(m)} &\triangleq \begin{bmatrix} a_1^{(m)} \\ \vdots \\ a_M^{(m)} \end{bmatrix}, \quad \boldsymbol{a}^{(m)} = \boldsymbol{O}^{m,\overline{m-1}} \cdot \boldsymbol{c}_{m-1}, \quad m = 2, \cdots, N \\ \boldsymbol{b}^{(m)} &\triangleq \begin{bmatrix} b_1^{(m)} \\ \vdots \\ b_M^{(m)} \end{bmatrix}, \quad \boldsymbol{b}^{(m)} = \boldsymbol{O}^{m,\bar{m}} \cdot \boldsymbol{c}_m. \quad m = 2, \cdots, N. \end{aligned} \tag{13b}$$

5. DISCUSSION

5.1. PECW/PMCW

In formulating CTMIE for 2-D dielectric waveguide devices we place two perfectly electric/magnetic conducting walls on top and bottom of

the structure. For waveguides with certain symmetry this is exactly what we want so that we may reduce the domain of the problem and cut down the computational costs. For open dielectric structures, the use of PECWs becomes an approximation. For an unbounded multi-layered waveguide, the modes are composed in terms of both discrete guiding modes and continuous radiation modes [25, 26]. The four **P Q R S** operators will be modified to include a summation term for the discrete spectrum and an integral term (with the upper limit extends to infinity) for the continuous spectrum. In theory we may do so. However, we will end-up with a much more complex formulation and an extremely difficult task of numerical implementation CTMIE solution. To check for numerical convergence or to study the effects of these two walls, we can either change the wall type or we can increase the distance between two walls.

5.2. Comparison with the MMM (Mode Matching Method)

CTMIE is a generalization of MMM [20]. They both apply stair-case approximation to the device under investigation. They both uses layer mode of the slices. MMM's unknowns are the coefficient vectors of slice modes in each slice, whereas in CTMIE, unknowns are interfacial field functions. The main difference is that MMM lacks the exact integral-equation formulation and the consequential benefits of it [18, 26, 27]. For some given problems when the fields are concentrated near the core region, CTMIE can choose some optimal expansion basis functions for the unknown tangential fields $\mathcal{E}_y(x)$ and $\mathcal{H}_y(x)$ using very few terms [18]. In essence, CTMIE uses far fewer unknowns than MMM would to obtain the same field solutions.

5.3. Choosing $N_b^{(m)}$, $M^{(m)}$ Parameters

In addition to N, the number of slice interface, there are two sets of important parameters in numerical solution of CTMIE namely $N_b^{(m)}$ and $M^{(m)}$. $N_b^{(m)}$ is used in Eq. (12a) to denote the number of terms used to expand the unknown field $\mathcal{H}_i(x)$. It is chosen to include all discrete guiding modes and some discretized radiation modes. $M^{(m)}$ is the number of layer modes used to represent the field solution in the mth slice. Under MMM, these numbers must be set to be the same.

$$N_b^{(m)} = M^{(m)} = M, \quad m = 1, \cdots, N+1 \quad \text{(MMM)}. \tag{14a}$$

The total unknowns are $2M \cdot N$ in mode matching method. In CTMIE each $N_b^{(m)}$ parameter can be independently chosen. The slice mode

number $M^{(m)}$ is chosen to be several time larger than interface basis number to have a good field match. Thus,

$$M^{(m)},\, M^{(m+)} \gg N_b^{(m)} \quad m = 1, \cdots, N. \quad \text{(CTMIE)}. \tag{14b}$$

6. CONCLUSIONS

In this paper, we have constructed a rigorous CTMIE formulation to study field solution of complex dielectric waveguide devices used in the planar lightwave circuit. In this formulation, a series of vertical cuts divide the waveguide device into a collection of dielectric slices made of horizontal layered. Within each slice four Green's kernels constructed from TE (or TM) layer modes map the unknown y-directed electric (or magnetic) field functions on the slice boundaries onto the x-component magnetic (or electric field). The continuity of these x-directed EM field component along each slice interface provide governing integral equations for the unknown interfacial functions $\mathcal{E}_y(x)$ (or $\mathcal{H}_y(x)$). To solve the unknown functions, we construct sets of suitable expansion functions and turn CTMIE into a coupled matrix equation which can be solve by a direct method optimized for banded structure. We leave the verification of our formulation as well as detail numerical discussion in future papers.

ACKNOWLEDGMENT

We are grateful to the support of the National Science Council of the Republic of China for financial support under the contracts NSC 95-2221-E-110-085 and NSC 96-2221-E-110-091. This work is also supported by the Ministry of Education, Taiwan under the Aim for the Top University Plan.

REFERENCES

1. Lin, C. F., *Optical Components for Communications*, Kluwer Academic Publishing, Boston, 2004.
2. Pavesi, L. and G. Guillot, *Optical Interconnects, the Silicon Approach*, Springer-Verlag, Berlin, 2006.
3. Chen, C. L., *Foundations for Guided-Wave Optics*, Wiley-Interscience, New Jersey, 2007.
4. Cheng, Y. H. and W. G. Lin, "Investigation of rectangular dielectric waveguides: an iteratively equivalent index method," *IEE Proc. Opto-Electron.*, Vol. 137, 323–329, 1990.

5. Lee, J. S. and S. Y. Shin, "On the validity of the effective-index method for rectangular dielectric waveguides," *J. Lightwave Technol.*, Vol. 11, 1320–1324, 1993.
6. Ishimaru, A., *Electromagnetic Propagation, Radiation, and Scattering*, Prentice Hall, Englewood Clifffs, N.J., 1991.
7. Cho, W.-C., *Waves and Fields in Inhomogeneous Media*, Van Norstrand Reinhold, New York, 1990.
8. Zhang, Y., W. Ding, and C. H. Liang, "Study on the optimum virtual topology for MPI based parallel conformal FDTD algorithm on PC clusters," *J. of Electromagn. Waves and Appl.*, Vol. 19, No. 13, 1817–1831, 2005.
9. Hwang, J.-N., "A compact 2-D FDFD method for modeling microstrip structures with nonuniform grids and perfectly matched layer," *IEEE Trans. Microwave Theory Tech.*, Vol. 53, No. 2, 2005.
10. Zheng, G., A. A. Kishk, A. W. Glisson, and A. B. Yakovlev, "A novel implementation of modified Maxwell's equations in the periodic finite-difference time-domain method," *Progress In Electromagnetics Research*, PIER 59, 85–100, 2006.
11. Hadi, M. F. and S. F. Mahmoud, "Optimizing the compact-FDTD algorithm for electrically large waveguiding structures," *Progress In Electromagnetics Research*, PIER 75, 253–269, 2007.
12. Chang, H.-W. and S.-M. Wang, "Large-scale hybrid FD-FD method for micro-ring cavities," *FWE6, Frontier in Optics*, 2005.
13. Fujisawa, T. and M. Koshiba, "A frequency-domain finite element method for modeling of nonlinear optical waveguide discontinuities," *IEEE PTL*, Vol. 16, No. 1, 2004.
14. Hernandez-Lopez, M. A. and M. Quintillan-Gonzalez, "A. finite element method code to analyse waveguide dispersion," *J. of Electromagn. Waves and Appl.*, Vol. 21, No. 3, 397–408, 2007.
15. Ooi, B. L. and G. Zhao, "Element-free method for the analysis of partially-filled dielectric waveguides," *J. of Electromagn. Waves and Appl.*, Vol. 21, No. 2, 189–198, 2007.
16. Yamauchi, J., *Propagating Beam Analysis of Optical Waveguides*, Research Studies Press, Baldock, England, 2003.
17. Scarmozzino, R., A. Gopinath, R. Pregla, and S. Helfert, "Numerical techniques for modeling guided wave photonic devices," *IEEE J. of Selected Topics in Quantum Electron.*, Vol. 6, 150–162, 2000.
18. Wu, T.-L. and H.-W. Chang, "Guiding mode expansion of a TE and TM transverse-mode integral equation for dielectric slab

waveguides with an abrupt termination," *J. Opt. Soc. Am. A*, Vol. 18, No. 11, 2823–2832, 2001.

19. Chang, H.-W., T.-L. Wu, and M.-H. Sheng, "Vectorial modal analysis of dielectric waveguides based on coupled transverse-mode integral equation: I - Mathematical formulations," *J. Opt. Soc. Amer. A*, Vol. 23, 1468–1477, 2006.
20. Chang, H.-W. and T.-L. Wu, "Vectorial modal analysis of dielectric waveguides based on coupled transverse-mode integral equation: II — Numerical analysis," *J. Opt. Soc. Amer. A*, Vol. 23, 1478–1487, 2006.
21. Itoh, T., *Numerical Techniques for Microwave and Millimeter-Wave Passive Structures*, Wiley Interscience, Signapore, 1989.
22. Huang, R. F. and D. M. Zhang, "Application of mode matching method to analysis of axisymmetric coaxial discontinuity in permeability permittivity measurement," *Progress In Electromagnetics Research*, PIER 67, 205–230, 2007.
23. Chang, H.-W. and W.-C. Cheng, "Analysis of dielectric waveguide termination with tilted facets by analytic continuity method," *J. of Electromagn. Waves and Appl.*, Vol. 21, No. 12, 1621–1630, 2007.
24. Berenger, J.-P., "A perfectly matched layer for the absorption of electromagnetic waves," *J. Comput. Phys.*, Vol. 114, No. 1, 185–200, 1994.
25. Yeh, P., *Optical Waves in Layered Media*, John Wiley & Sons, New York, 1991.
26. Sabetfakhri, K. and L. P. B. Katehi, "An integral transform technique for analysis of planar dielectric structures," *IEEE Trans. Microwave Theory Tech.*, Vol. 42, 1052–1062, 1994.
27. Sabetfakhri, K. and L. P. B. Katehi, "An integral transform technique for analysis of planar dielectric structures," *IEEE Trans. Microwave Theory Tech.*, Vol. 42, 1052–1062, 1994.
28. Tong, M. S., "A stable integral equation solver for electromagnetic scattering by large scatterers with concave surface," *Progress In Electromagnetics Research*, PIER 74, 113–130, 2007.